Pergamon

Bioorganic & Medicinal Chemistry 9 (2001) 1045–1057

BIOORGANIC & MEDICINAL CHEMISTRY

Synthesis, Pharmacological Characterization and QSAR Studies on 2-Substituted Indole Melatonin Receptor Ligands

Marco Mor,[a] Gilberto Spadoni,[b,*] Barbara Di Giacomo,[b] Giuseppe Diamantini,[b] Annalida Bedini,[b] Giorgio Tarzia,[b] Pier Vincenzo Plazzi,[a] Silvia Rivara,[a] Romolo Nonno,[c] Valeria Lucini,[c] Marilou Pannacci,[c] Franco Fraschini[c] and Bojidar Michaylov Stankov[c]

[a]*Dipartimento Farmaceutico, Università degli Studi di Parma, Parco Area delle Scienze 27A, I-43100 Parma, Italy*
[b]*Istituto di Chimica Farmaceutica e Tossicologica, Università degli Studi di Urbino, Piazza Rinascimento 6, I-61029 Urbino, Italy*
[c]*Cattedra di Chemioterapia, Dipartimento di Farmacologia, Università degli Studi di Milano, Via Vanvitelli 32, I-20129 Milano, Italy*

Received 1 August 2000; revised 22 November 2000; accepted 28 November 2000

Abstract—A number of 6-methoxy-1-(2-propionylaminoethyl)indoles, carrying properly selected substituents at the C-2 indole position, were prepared and tested as melatonin receptor ligands. Affinities and intrinsic activities for the human cloned mt_1 and MT_2 receptors were examined and compared with those of some 2-substituted melatonin derivatives recently described by us. A quantitative structure–activity relationship (QSAR) study of the sixteen 2-substituted indole compounds, **5a–k**, **1**, **8–11**, using partial least squares (PLS) and multiple regression analysis (MRA) revealed the existence of an optimal range of lipophilicity for the C-2 indole substituent. There are also indications that planar, electron-withdrawing substituents contribute to the affinity by establishing additional interactions with the binding pocket. No mt_1/MT_2 subtype selectivity was observed, with the relevant exception of the 2-phenethyl derivative **5e**, which exhibited the highest selectivity for the h-MT_2 receptor among all the compounds tested (MT_2/mt_1 ratio of ca. 50). Conformational analysis and superposition of **5e** to other reported selective MT_2 ligands revealed structural and conformational similarities that might account for the MT_2/mt_1 selectivity of **5e**.

Introduction

Melatonin (*N*-acetyl-5-methoxytryptamine, MLT, **1**) is the principal hormone secreted by the pineal gland during the dark period of the light/dark cycle.[1] MLT influences a variety of functions such as seasonal reproduction in photoperiodic animals, circadian rhythms, sleep processes, immune functions, thermoregulation, oxidant/antioxidant balance, cancer biology, and others.[2] Although its exact role in humans still remains unclear, research on MLT suggests possible clinical implications, especially in the treatment of circadian-rhythm-based sleep disorders.[3–7] Protective effects on the cardiovascular system by reducing the risk of atherosclerosis and hypertension[8] have also been reported. The potential therapeutic implications of MLT justify the considerable efforts devoted to understand how MLT interacts with its receptors.

Most of the functions of MLT in vertebrates are mediated by the action of MLT on specific high-affinity membrane receptors,[9–12] recently classified as mt_1, MT_2, putative MT_3 and Mel1c.[13] Mel1c is found only in lower vertebrates and birds while mt_1 and MT_2 have been found in higher vertebrates and humans.

Previous extensive studies on indole derivatives and indole bioisosteres of MLT demonstrated that suitably spaced methoxy and amido moieties are important for binding to and activation of the melatonin receptor.[14,15] To improve the information about the essential pharmacophoric features of the MLT molecule, and to establish which regions can tolerate structural modulation, we have described several indole compounds exhibiting affinity and intrinsic activity for the melatonin receptors to varying degrees.[16,17] Numerous conformationally constrained MLT analogues have also been synthesized and tested to elucidate the bioactive conformation of MLT (for extensive reviews see refs. 14,15,18). Starting from these studies, we and other authors have recently

*Corresponding author. Tel.: +39-722-2545; fax: +39-722-2737; e-mail: gilberto@uniurb.it

0968-0896/00/$ - see front matter
PII: S0968-0896(00)00322-9

proposed molecular models of the putative melatonin binding site (for a review see ref. 15).

Although the limited series of the known 2-substituted compounds suggested that C-2 halogens or phenyl group[19–21] contribute significantly to the receptor binding, a systematic investigation on the relevance of this C-2 substituent is lacking. The modulatory effect on affinity had been previously ascribed to the influence of the C-2 substituent on the ethylamido side chain folding.[22] However, the remarkable increase in binding affinity observed in 2-substituted rigid melatonergic ligands favours the existence of an auxiliary binding site around the C-2 indole position.[23] Increased binding affinity and MT_2 selectivity were also observed in some melatonin antagonists/partial agonists, by introducing a benzyl or a phenyl group at the C-2 indole or in a topologically equivalent position.[24,25]

In a previous paper,[26] we reported that the shift of the MLT side chain from C-3 to N-1 indole position affords a series of melatonin bioisosteres (**II**) with affinity and SAR comparable to that of the natural melatonin series, provided that the methoxy group is in the C-6 indole position.

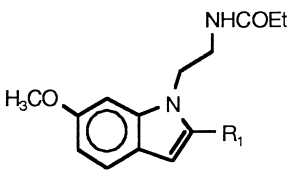

5a-k

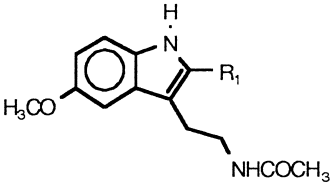

1, 8-11

In our continuing interest in the characterization of MLT receptors, we have further synthesized and pharmacologically characterized new 2-substituted MLT-bioisosteres (**II**) in order to get quantitative correlations, explaining the dependence of the biological activity and mt_1/MT_2 selectivity on the physicochemical features of the C-2 indole substituent. Substituents were chosen to provide both a broad distribution of physicochemical properties (lipophilicity and electronic and steric effects) and minimal cross-correlation. Their selection was based on substituent properties, synthetic feasibility and on previously reported 2-substituted MLT analogues.[24,27,28] Three disjoint principal properties (DPPs), obtained by van de Waterbeemd et al.[29] from an extended set of variables for 59 substituents, were employed for a concise description of physicochemical properties necessary for an optimization study.[30] Starting from a putative 'optimal' set of substituents, composed by the eight combinations of high and low levels for each property (corresponding to a factorial design[31]), substituent replacements and additions were performed (see Experimental).

The pharmacological results of the corresponding derivatives, synthesized and tested on mt_1 and MT_2 melatonin receptor subtypes, are presented in Table 1, and the correlation matrix of their DPPs is reported in Table 2.

Selectivity toward mt_1 and MT_2 melatonin receptor subtypes was also investigated; finally molecular modeling was employed to investigate the steric features of the most flexible substituents which showed some MT_2 selectivity.

Results

The goal of this study was to prepare a series of 2-substituted-1-(2-propionylaminoethyl)indoles (Schemes 1 and 2) and to measure their affinity and efficacy at the h-mt_1 and h-MT_2 receptors (Table 1). A total of 16 compounds were then examined in a quantitative structure–activity relationship (QSAR) analysis (Tables 3 and 5) to investigate quantitatively the effect of properly selected lipophilic and hydrophilic C-2 substituents on melatonin receptor affinity, efficacy and selectivity.

Chemistry

The 2-substituted melatonin analogues **8**–**9**[19,20] and related bioisosters **5a**–**k** (Table 1) were synthesized by known chemical processes. The general synthetic route involved an intermediary 2-substituted-5- or 6-methoxy indole. Some of these indoles were prepared according to previously described procedures (**2a**,[32] **2b**,[33] and **2d**[25]). By reacting 6-methoxy-1H-indole with dimethyldisulfide and sulfonylchloride, according to a method previously described for related compounds,[34] we obtained a mixture of mono- and bis-methylthio indole isomers that was converted to 6-methoxy-2-methylthio-1H-indole by acid-catalyzed isomerization with polyphosphoric acid (PPA) at 100 °C. The thiomethyl group was then readily oxidized to 2-methanesulfonyl-1H-indole (**2c**) with magnesium monoperoxyphtalate hexahydrate (MMPP) under biphasic conditions (H_2O/CH_2Cl_2/benzyltriethylammonium chloride).

A literature procedure[26] (Scheme 1) was used for the synthesis of *N*-[2-(2-substituted-6-methoxy-1*H*-indol-1-yl)-ethyl]propionamido derivatives (**5a**–**c**, **e**). *N*-cyanomethylation of indoles **2a**–**d** with sodium hydride and chloroacetonitrile in DMF gave the required 1-cyanomethylindoles **3a**–**d**. Intermediates **3a**–**c** were converted to the final compounds **5a**–**c** by hydrogenation over Raney nickel and concomitant *N*-acylation with propionic anhydride. Aldehyde **3d** was subjected to Wittig reaction conditions[35] using benzyltriphenylphosphonium chloride in the presence of 1,7-diazabicyclo[4.5.0.]undec-6-ene (DBU) to give an E/Z mixture of the 2-styryl derivative **4** which was converted to the 2-phenethyl derivative **5e** by hydrogenation over Raney nickel and concomitant *N*-acylation with propionic anhydride. (In some cases it was necessary to terminate the reduction of the styryl group by catalytic hydrogenation with 10% palladium over carbon at room temperature for 16 h.)

1-(2-Propionylamino-ethyl)-6-methoxy-1*H*-indol-1-yl-2-carboxylic acid **6**, obtained by alkaline ester hydrolysis of **5a**, was reacted with thionyl chloride in dry tetrahydrofuran (THF) and the crude acid chloride was treated with a saturated solution of ammonia in dichloromethane

Table 1. Binding affinity[a] and intrinsic activity of MLT and compounds **5a–k**, **8–11** for the human mt_1 or MT_2 melatonin receptors stably expressed in NIH3T3 cells

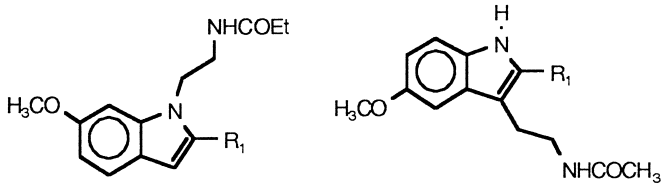

5a-k **1, 8-11**

Compd.	R_1	Human mt_1		Human MT_2		$pK_{i1}-pK_{i2}$[c]
		pK_i ±SEM	Relative intrinsic activity[b]	pK_i ±SEM	Relative intrinsic activity[b]	
5a	COOMe	9.82±0.07	0.98±0.02	10.12±0.05	1.33±0.08	−0.30
5b	CF_3	9.52±0.12	0.83±0.01	10.08±0.12	1.02±0.06	−0.56
5c	SO_2Me	6.83±0.07	0.79±0.01	7.34±0.13	0.78±0.07	−0.51
5d	CHO	8.95±0.04	0.98±0.05	9.34±0.05	1.11±0.06	−0.39
5e	CH_2CH_2Ph	7.20±0.07	0.75±0.01	8.88±0.12	0.27±0.05	−1.68
5f	$CONH_2$	7.57±0.07	0.98±0.02	7.79±0.08	1.02±0.07	−0.22
5g	$NHCONH_2$	6.65±0.03	0.89±0.04	7.21±0.15	0.72±0.07	−0.56
5h	CH_2OH	7.46±0.0	0.96±0.04	7.87±0.05	0.94±0.01	−0.41
5i	H	8.77±0.09	0.93±0.06	9.21±0.09	1.03±0.07	−0.44
5j	Ph	9.97±0.05	0.92±0.03	10.36±0.09	1.17±0.01	−0.38
5k	Br	10.28±0.03	0.95±0.01	10.21±0.06	1.27±0.08	+0.07
MLT (**1**)	H	9.63±0.03	1	9.43±0.03	1	+0.20
2-BrMLT (**8**)	Br	10.54±0.04	0.98±0.01	9.94±0.06	1.05±0.02	+0.60
2-PhMLT (**9**)	Ph	10.66±0.06	0.96±0.01	10.42±0.07	0.98±0.01	+0.24
2-IMLT (**10**)	I	10.64±0.03		10.29±0.05	1.02±0.01	+0.35
2-BnMLT (**11**)[d]	CH_2Ph	7.5[d]		9.6[d]		−2.10

[a]pK_i values were calculated from IC_{50} values obtained from competition curves by the method of Cheng and Prusoff[40] and are the means of at least three independent determinations performed in duplicate.
[b]The relative intrinsic activity values were obtained by dividing the maximal analogue-induced G-protein activation by that of MLT.
[c]The difference ($pK_{i1}-pK_{i2}$) represents selectivity towards the mt_1 (positive values) or the MT_2 (negative values) subtype.
[d]pK_i values from ref 24.

Table 2. Correlation matrix for disjoint principal properties of 2-substituents in compounds **5a–k**

	S_1	L_1	E_1
S_1	1.00	0.45	0.04
L_1	0.45	1.00	0.40
E_1	0.04	0.40	1.00

to yield the 2-carboxylic acid amide derivative **5f** (Scheme 2). The acid **6** was subjected to a modified Curtius reaction[36] to obtain the carbonylazido derivative **7**. Treatment of **7** with ammonium acetate in refluxing toluene provided the 2-ureido derivative **5g** (Scheme 2).

The 2-carboxymethyl derivative **5a** was reduced by $LiAlH_4$ to the hydroxymethyl derivative **5h**, that was oxidized by MnO_2 to the 2-carboxaldehyde derivative **5d** (Scheme 2).

Pharmacology

Evaluation of the compounds was performed by measuring the melatonin receptor binding affinity and in vitro functional activity.

The binding affinity of compounds **5a–k** was determined using 2-[^{125}I]iodomelatonin (100 pM) as a labelled ligand in competition binding analyses on cloned human mt_1 and MT_2 receptor subtypes stably expressed in NIH3T3 rat fibroblast cells and the results are summarized in Table 1. The characterization of NIH3T3-mt_1 and MT_2 cells was described in detail elsewhere.[28,37]

The activation of the G-protein subsequent to the binding of compounds **5a–k** to mt_1 and MT_2 receptor subtypes was determined by measuring the specific binding of [^{35}S]-guanosine-5′-(3-thiotriphosphate) ([^{35}S]GTPγS) to membranes prepared from NIH3T3 cells expressing human cloned mt_1 or MT_2 melatonin receptors. The detailed description and validation of this method was reported elsewhere.[25,28,37] In both human mt_1 and MT_2 receptor-expressing cell lines, MLT produced a concentration-dependent stimulation of basal [^{35}S]GTPγS binding with a maximal stimulation of 370% in mt_1 and 250% in MT_2 above basal levels, respectively. The amount of bound [^{35}S]GTPγS is proportional to the level of the analogue-induced G-protein activation, and it is related to the intrinsic activity of the compounds. Full agonists increased the basal [^{35}S]GTPγS binding in a concentration-dependent manner, likewise the natural ligand MLT, whereas partial agonists increased it to a much lesser extent than MLT and antagonists were without any effect. The relative intrinsic activity values were obtained by dividing the maximal G-protein activation of a test compound by that of MLT and the results are summarized in Table 1.

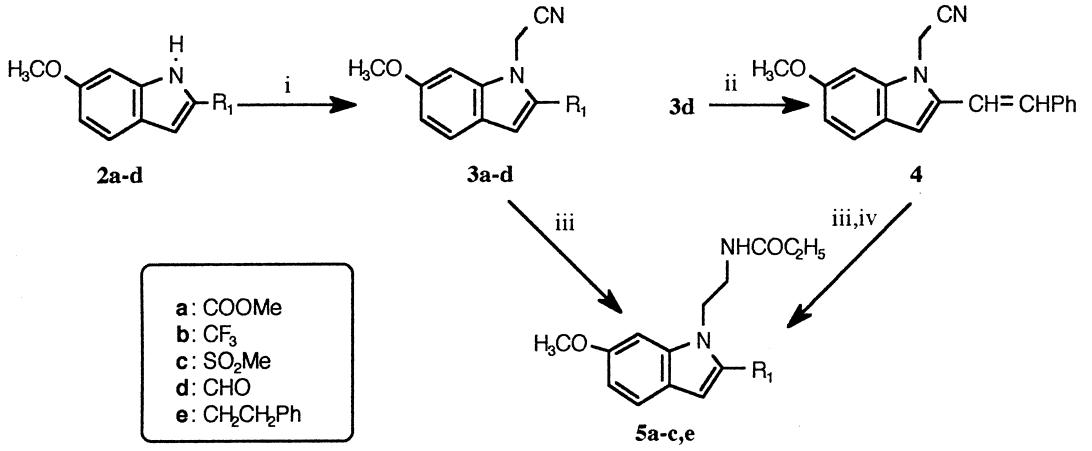

Scheme 1. Reagents and conditions: (i) NaH, $ClCH_2CN$, DMF, room temperature, 16 h; (ii) $(Ph)_3P^+CH_2C_6H_5Cl^-$, DBU, toluene, reflux, 4 h; (iii) Raney nickel, H_2, 4 atm, $(EtCO)_2O$, THF, 50 °C, 6 h (24 h for **5e**); (iv) Pd-C, H_2, THF, room temperature, 16 h.

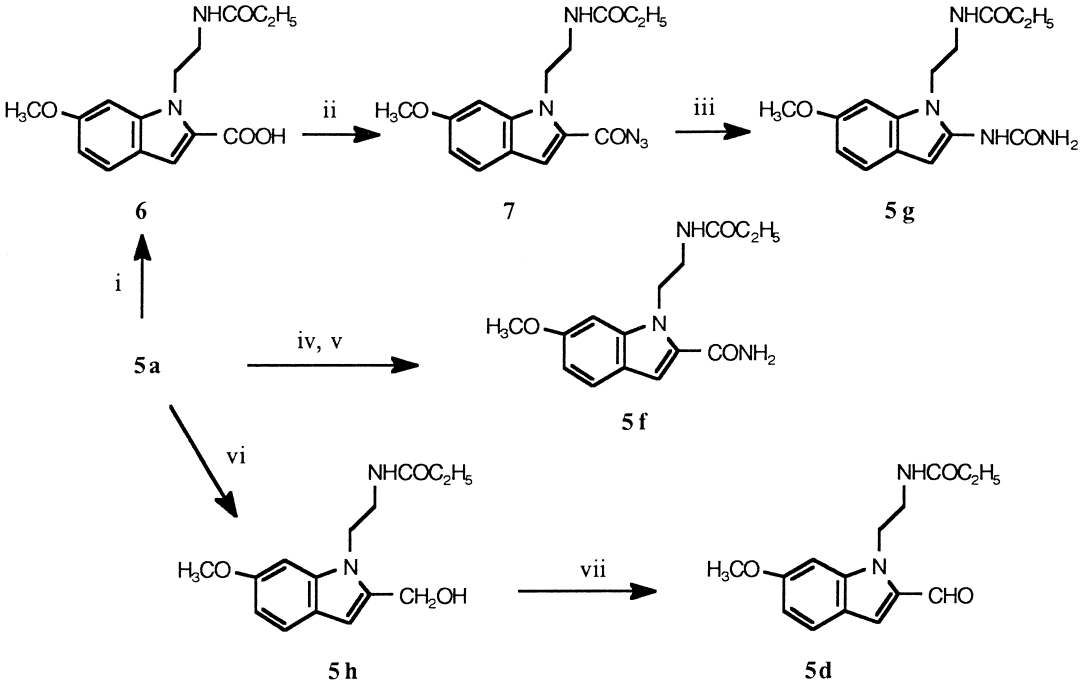

Scheme 2. Reagents and conditions: (i) 3 N KOH, MeOH, THF, room temperature, 16 h; (ii) $(PhO)_2P(O)N_3$, Et_3N, benzene, room temperature, 24 h; (iii) $CH_3COO^-NH_4^+$, toluene, reflux, 5 min; (iv) $SOCl_2$, THF, 50 °C, 4 h; (v) NH_3, CH_2Cl_2/THF, room temperature, 2 h; (vi) $LiAlH_4$, THF, 10 °C, 1 h; (vii) MnO_2, CH_2Cl_2, room temperature, 7 h.

QSAR

Relationship between mt_1 and MT_2 affinity. As can be observed from Figure 1, representing pK_i values of compounds **5a–k** for the two receptor subtypes, the affinity for MT_2 receptor is strictly correlated with that for mt_1 one. A relevant exception is the phenethyl derivative **5e**, which shows much lower affinity for mt_1 receptor than the parent compound **5i**, but almost the same affinity as **5i** for MT_2 receptor. Another feature of this compound, partially shared by the methylsulphonyl derivative **5c**, is its low intrinsic activity on cells expressing MT_2 receptor subtype. Excluding from the correlation the outlier **5e**, the following regression equation can be obtained:

$$pK_i\ (MT_2) = 0.93(\pm 0.04)\ pK_i\ (mt_1) + 0.97(\pm 0.37)$$
$$n = 10 \quad R^2 = 0.98 \quad s = 0.17 \quad F = 476. \qquad (1)$$

The positive intercept indicates that pK_i values on the MT_2 subtype are slightly, but systematically, higher than on the mt_1 one. This systematic difference is not observed for MLT derivatives **8–10**, as can be seen from Table 1.

Multiple regression analysis (MRA). No single variable, among those reported in Table 3, provided a statistically good linear model either for mt_1 or for MT_2 receptor binding affinity, whereas a parabolic relationship between the logarithm of the relative affinities (pRA1

Table 3. Regression analysis (eqs (7) and (8)) of structure-relative binding affinity (pRA1, pRA2) of 2-substituted-1-(2-propionylaminoethyl)indoles (**5a–k**), MLT (**1**) and 2-melatonin derivatives (**8–11**)

Compd	Subst.	pRA1			pRA2		
		Obs.	Calc.[a]	Res.	Obs.	Calc.[b]	Res.
5a	COOMe	1.05	0.82	0.23	0.91	0.49	0.42
5b	CF_3	0.75	1.34	−0.59	0.87	1.09	−0.22
5c	SO_2Me	−1.94	−1.54	−0.40	−1.87	−1.65	−0.22
5d	CHO	0.18	0.02	0.16	0.13	−0.25	0.38
5e	CH_2CH_2Ph	−1.57	−1.24	−0.33	−0.33	−0.16	−0.17
5f	$CONH_2$	−1.2	−1.71	0.51	−1.42	−1.69	0.27
5g	$NHCONH_2$	−2.12	−1.95	−0.17	−2.00	−1.75	−0.25
5h	CH_2OH	−1.31	−1.35	0.04	−1.34	−1.26	−0.08
5i	H	0.00	0.05	−0.05	0.00	0.01	−0.01
5j	Ph	1.20	0.04	1.16	1.15	0.52	0.63
5k	Br	1.51	1.26	0.25	1.00	1.03	−0.03
1 (MLT)		0.00	0.05	−0.05	0.00	0.01	−0.01
8 (2-BrMLT)		0.91	1.26	−0.35	0.51	1.03	−0.52
9 (2-PhMLT)		1.03	0.04	0.99	0.99	0.52	0.47
10 (2-IMLT)		1.01	1.15	−0.14	0.86	1.04	−0.18
11 (2-BnMLT)[c]		−1.57	−0.31	−1.26	−0.14	0.32	−0.46

[a]From eq (7).
[b]From eq (8).
[c]Calculated from K_i values reported by ref 24 for Mel_{1a} (2-BnMLT: 32.7 nM, MLT: 0.88 nM) and Mel_{1b} (2-BnMLT: 0.25 nM, MLT: 0.18 nM) receptors expressed in COS-7 cellular lines.

Table 4. Structural descriptors employed for QSAR analysis[29]

π	Aromatic substituent constants for lipophilicity
MR	Molar refractivity
L	Second generation length STERIMOL parameter
B1	Second generation minimum width STERIMOL parameter
B5	Second generation maximum width STERIMOL parameter
Sb	Austel's steric branching parameter
σ_m	Hammett constant for *meta* substitution
σ_p	Hammett constant for *para* substitution

and pRA2) and lipophilicity can be recognized from Figure 2, and can be expressed by the following equations:

$$\text{pRA1} = 0.90(\pm0.17)\ \pi - 0.58(\pm0.12)\ \pi^2 + 0.74(\pm0.30)$$
$$n = 11 \quad R^2 = 0.80 \quad s = 0.67 \quad F = 16.5 \quad Q^2 = 0.38$$
$$\text{SDEP} = 1.01 \quad \text{Optimal } \pi = 0.78 \qquad (2)$$

$$\text{pRA2} = 0.93(\pm0.12)\ \pi - 0.43(\pm0.08)\ \pi^2 + 0.51(\pm0.20)$$
$$n = 11 \quad R^2 = 0.89 \quad s = 0.46 \quad F = 31 \quad Q^2 = 0.74$$
$$\text{SDEP} = 0.59 \quad \text{Optimal } \pi = 1.08 \qquad (3)$$

These equations can explain 80% and 89% of the total variation in the dependent variable, respectively, as expressed by the square of the correlation coefficient, R^2 values; the standard error of the residuals (s) is rather large in both cases, if compared to the uncertainty of the affinity values on log scale (a difference of 0.3 corresponds to a doubling of K_i), but the F values, being significantly higher than 1, allow to exclude, with good confidence, the hypothesis of chance correlation.

Although a biphasic profile of these relationships is evident, eq (2) lacks a good predictive power (Q^2, see Experimental for a definition), as the low affinity of the phenethyl derivative **5e** suggests rather a cut-off value than a parabolic trend, and the good performance of the phenyl substituent seems to be underestimated. On the other hand, eqs (2) and (3) represented by far the best two-variable regression models both for pRA1 and pRA2. Therefore, whereas other structural properties are supposed to play a role, their influence is statistically shadowed by the parabolic correlation.

Table 5. Descriptive (R^2) and predictive (Q^2) power of PLS models with increasing number of latent variables (LV); weights of physicochemical properties (W_X) and of relative binding affinity (C) in each LV

LV	1st	2nd	3rd	4th
R^2X	0.306	0.607	0.789	0.929
R^2Y	0.612	0.832	0.864	0.895
Q^2	0.401	0.645	0.645	0.687
W_X				
π	0.495	0.590	0.013	−0.171
MR	−0.064	0.493	−0.063	0.101
L	−0.053	0.456	0.005	0.301
B1	0.295	0.044	−0.757	0.191
B5	−0.323	0.266	0.031	0.103
Sb	−0.304	0.180	0.229	0.548
σ_m	0.269	−0.220	−0.226	0.430
σ_p	0.182	−0.216	0.163	0.579
π^2	−0.598	0.017	−0.541	−0.048
C				
pRA1	0.605	0.190	0.141	0.152
pRA2	0.513	0.364	0.280	0.186

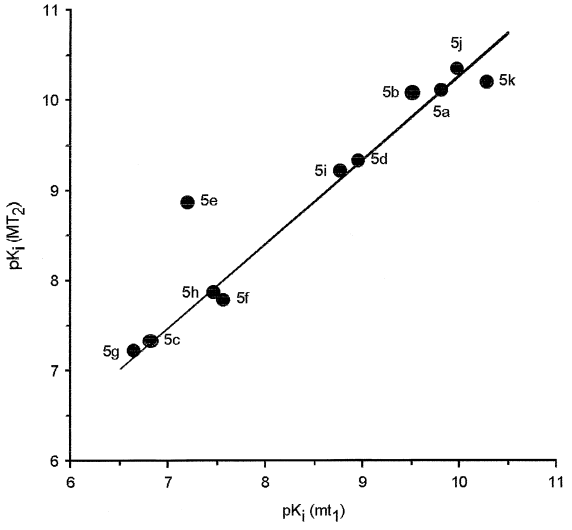

Figure 1. Relationship between mt_1 and MT_2 affinity for compounds **5a–k**. The line represents eq (1) (see text).

The best three-variable MRA models were those including, in addition to lipophilicity, the electronic effect of the substituent, without strong differences between σ_m and σ_p. Eqs (4) and (5), using σ_m are reported, but similar correlation could also be obtained with σ_P.

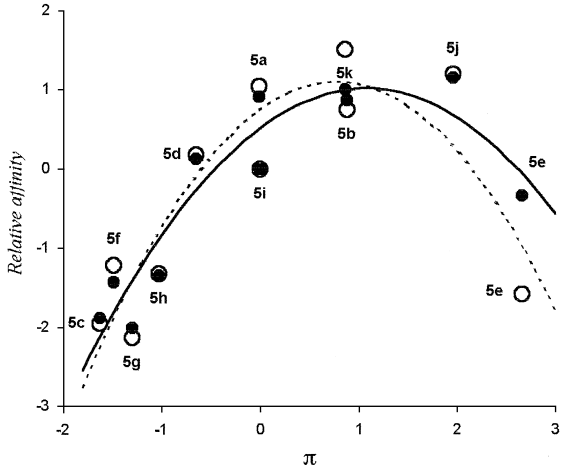

Figure 2. Relative affinity of compounds **5a**–**k** versus lipophilicity. Hollow circles: pRA1; filled circles: pRA2; dotted line: eq (2); continuous line: eq (3).

$$\text{pRA1} = 0.93(\pm0.15)\,\pi - 0.51(\pm0.11)\,\pi^2 + 1.81(\pm0.90)\,\sigma_m + 0.23(\pm0.36)$$
$$n = 11 \quad R^2 = 0.88 \quad s = 0.57 \quad F = 16.5 \quad Q^2 = 0.53$$
$$\text{SDEP} = 0.88 \qquad (4)$$

$$\text{pRA2} = 0.95(\pm0.09)\,\pi - 0.37(\pm0.07)\,\pi^2 + 1.41(\pm0.56)\,\sigma_m + 0.11(\pm0.22)$$
$$n = 11 \quad R^2 = 0.94 \quad s = 0.35 \quad F = 36.6 \quad Q^2 = 0.83$$
$$\text{SDEP} = 0.47 \qquad (5)$$

Although the introduction of the electronic variable improved the predictive power, compound **5e** remained a severe outlier in these models, and it can be suspected to affect the analysis for its excessive leverage. Its exclusion from the test set caused a high correlation between the two biological variables (see above) leading to very similar QSARs for pRA1 and pRA2; for this reason, only the equations involving pRA2 are further discussed.

In spite of the exclusion of the most lipophilic substituent (**5e**), the parabolic dependence of affinity on lipophilicity was still observed, as illustrated by eq (6), indicating that this trend did not depend only on the loss of affinity observed for **5e**. In eq (6) the Q^2 value is closer to the R^2 one, indicating that the ability of the model to explain pRA2 variation is similar in prediction and in calculus, and that no compound is influencing the model with an excessive leverage.

$$\text{pRA2} = 0.98(\pm0.12)\,\pi - 0.32(\pm0.12)\,\pi^2 + 0.40(\pm0.21)$$
$$n = 10 \quad R^2 = 0.91 \quad s = 0.44 \quad F = 34.2 \quad Q^2 = 0.84$$
$$\text{SDEP} = 0.48 \quad \text{Optimal } \pi = 1.53 \qquad (6)$$

A comparison of the effects of 2-substituents on the melatonin scaffold can be attempted, considering the logarithm of relative affinity data (pRA) of MLT derivatives **8**–**11** (Table 3). The benzyl derivative of MLT (5-methoxyluzindole, **11**) behaved as **5e**, being much less potent on mt_1 receptor than on MT_2 in displacing the labelled ligand.

In the 16-compound set, comprising MLT derivatives, parabolic relationships between relative affinity and lipophilicity could still be observed, and electron-withdrawing effects (described by either σ_m or σ_p) improved the fitting.

$$\text{pRA1} = 0.87(\pm0.15)\,\pi - 0.48(\pm0.11)\,\pi^2 + 2.10(\pm0.89)\,\sigma_m + 0.05(\pm0.34)$$
$$n = 16 \quad R^2 = 0.79 \quad s = 0.65 \quad F = 15.1 \quad Q^2 = 0.64$$
$$\text{SDEP} = 0.74 \qquad (7)$$

$$\text{pRA2} = 0.89(\pm0.09)\,\pi - 0.34(\pm0.06)\,\pi^2 + 1.31(\pm0.51)\,\sigma_m + 0.01(\pm0.20)$$
$$n = 16 \quad R^2 = 0.90 \quad s = 0.38 \quad F = 36.4 \quad Q^2 = 0.84$$
$$\text{SDEP} = 0.42 \qquad (8)$$

As in the case of the **5a**–**k** set, the correlation is slightly better for pRA2 values; the pRA1 value of 2-benzyl-MLT was overestimated (thus leading to a decrease of Q^2), while the contribution to mt_1 affinity of the phenyl group was underestimated for both **5j** and 2-PhMLT. It is worth noting that the coefficients of eqs (8) and (5) are very similar, thus suggesting that electron-withdrawing substituents with an optimal lipophilicity (π value around 1) should lead to better affinity, and that this QSAR is common to the whole series of indole derivatives. Observing the residuals, reported in Table 3, it can also be inferred that this simple regression model underestimates the affinity contribution of planar substituents having π-electron clouds (i.e., phenyl group, and substituents with a carbonyl group directly attached to the indole ring), giving positive residuals for them. This feature could not be accounted for by the electronic descriptors employed, and a similar result occurred with σ_p instead of σ_m.

Partial least squares projections to latent variables (PLS analysis)

PLS has the advantage, over MRA, that the variables in the Y matrix (pRA) are correlated with latent variables (LV), calculated from the X matrix, which are mutually orthogonal; the LVs can therefore be regarded as describing statistically independent effects of the physicochemical properties on the biological ones.

In the PLS analysis, pRA1 and pRA2 were used as the Y matrix, and the eight variables reported in Table 4, plus a squared expansion of π (π^2), as the X matrix. When the 11 compounds **5a**–**k** were considered, no simple PLS model with appreciable predictive power (at cross-validation) could be achieved. Including MLT (**1**) and the MLT derivatives **8**–**11**, the increased number of compounds (16) led to an improvement in the statistics of the PLS model. R^2, Q^2, and the PLS weights (W_X) of

the PLS model obtained are reported in Table 5 for the first four latent variables (LV). The PLS weights allow the calculation of the coordinates on the latent variables (scores, t) from the X matrix: $\mathbf{T}=\mathbf{X}\times\mathbf{W_X}$; the W_X values can therefore be used to explain the chemical meaning of the latent variables, considering that the calculated Y values are obtained as $\mathbf{Y}=\mathbf{T}\times\mathbf{C}$, where C are the coefficients relating each Y variable to each LV.

The first two LVs describe the most relevant effects of physicochemical properties on affinity, as they improve the predictive power of the model (Q^2) and explain 83% of pRA variation, with an R^2 in the X space of 0.607 (i.e., they use 60.7% of the whole variance of the X matrix). The first LV is dominated by the parabolic effect of lipophilicity, as argued by the W_X values of π and π^2; the second one, which has a stronger influence on pRA2 than on pRA1, is mainly due to a linear effect of lipophilicity, and can be explained by the fact that more lipophilic substituents are more tolerated by MT_2 receptor. The next two LVs should be inspected looking for additional effects, even if they could not significantly improve the predictive power, and each of them could explain only an additional 3% of Y variation. The third LV, which is still more related to pRA2 than to pRA1, gives the highest weight to the Verloop minimum-width parameter (B1); the negative sign means that better affinity can be obtained for substituents with small B1, that is the planar ones. The fourth LV contains electronic information, meaning that electron-withdrawing substituents have a positive influence both on pRA1 and pRA2.

Molecular modeling

The conformational analysis performed on the phenethyl group of **5e** and the benzyl group of **11** showed that, superposing the putative pharmacophore elements of MLT receptor ligands, as defined in ref 23, the C-2 ending phenyl ring of the two compounds can occupy the same position, lying out of the plane of the indole ring.

Table 6 reports the distances among some key features for the couples of conformers having differences in those distances lower than 1 Å, corresponding to different superposition models. Those referred as superposition 1 and 3 (Fig. 3), correspond to the arrangement of the phenyl ring of the C-2 substituent above and below the plane of the indole ring, respectively. These two models also allow the superposition of the known MT_2 selective antagonist 4-phenyl-2-acetylamino-tetralin (4-P-ADOT, not shown), which has the phenyl ring attached to a tetrahedral carbon, and thus projected out of the plane of the tetralin nucleus; the same was not possible for superposition 2, presenting the phenyl ring of the 2-substituent too close to the acylaminoethyl chain.

Table 6. Distances (Å) between the phenyl ring in position 2 and other key features for minimum-energy conformations of **5e** and **11** which can be superposed

		5e	11
Superposition 1			
	Amide O[a]	7.39	7.31
	Amide H[b]	7.92	7.46
	Indole benzene[c]	6.02	6.26
	Height above the plane[d]	2.81	2.21
Superposition 2			
	Amide O[a]	3.81	3.59
	Amide H[b]	4.00	4.60
	Indole benzene[c]	6.45	6.34
	Height above the plane[d]	3.29	2.46
Superposition 3			
	Amide O[a]	9.48	9.06
	Amide H[b]	7.88	7.32
	Indole benzene[c]	5.53	6.30
	Height above the plane[d]	−3.04	−2.60

[a]Distance between the centroid of the phenyl ring in position 2 and the amide oxygen.
[b]Distance between the centroid of the phenyl ring in position 2 and the amide hydrogen.
[c]Distance between the centroid of the phenyl ring in position 2 and the centroid of the benzene fragment of the indole nucleus.
[d]Distance between the centroid of the phenyl ring in position 2 and the plane of the indole ring; a positive value means that the phenyl ring points to the same direction as the acylaminoethyl side chain.

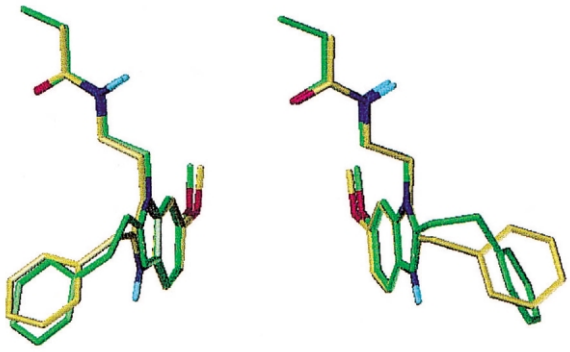

Figure 3. Superpositions 1 (left) and 3 (right) of **5e** (green carbons) and **11** (yellow carbons) as described in Table 6. The arrangement of the phenyl rings out of the plane of the indole nucleus is evidenced. Non-carbon atoms are color coded.

Discussion

It is apparent from the data presented in Table 1 that 2-substituted indole melatonergic ligands bind at h-mt_1 or h-MT_2 receptors with varying affinity. Lipophilicity of the 2-substituent is clearly the major determinant for mt_1 and MT_2 affinity, as its parabolic relationship explains most of the affinity variation, and additional effects can hardly be observed with sufficient statistical significance. However, the relatively high residuals of the corresponding models (eqs (2) and (3)) indicate that other structural features are playing a role in receptor binding. In fact, from MRA and PLS models, indications arise that planar, electron-withdrawing substituents can establish additional interactions with the binding pocket.

The QSARs observed for the substituents at the 2 position of 1-acylaminoethylindoles seem to be followed also by the corresponding MLT derivatives **8**–**11**, at least for the few data on cloned receptors available so

far (see eqs (7) and (8)). Binding data on native tissues, with heterogeneous populations of receptor subtypes, have been reported for some 2-alkyl-MLT derivatives: while in 2-methyl-MLT a small increase in affinity had been achieved, both *iso*-propyl and cyclohexyl substituents had led to a drop of affinity.[20] This behavior can qualitatively be compared to the QSARs reported above, suggesting that branched alkyl substituents could be detrimental for receptor binding, in spite of positive lipophilic contribution, due to their electronic features and non-planar shape.

The descending branches of the parabolic relations, illustrated in Figure 2, represent the main difference between mt_1 and MT_2 SARs; as this is mainly due to the phenethyl group of **5e**, it can be attributed to higher steric tolerance of the MT_2 subtype. In fact, the effect of the phenethyl substituent (**5e**), leading to a drop of affinity which is much higher on the mt_1 than on the MT_2 receptor, points out to a different shape for the two binding pockets. On the other hand, for **5e**, and for the other non-planar substituent of **5c**, a higher depression of MT_2 intrinsic activity is observed on the cellular line employed; this behavior recalls that of 5-methoxyluzindole (**11**) and of 4-phenyl-2-acetyl-amino-tetralin (4-P-ADOT) derivatives, which have been found to display good selectivity for the MT_2 receptor subtype, with low intrinsic activity.[24]

Molecular models of **5e** and **11** indicated that the ending phenyl ring of the two compounds can be superposed out of the plane of the indole nucleus, either above or below it (see Fig. 3); this is also possible for 4-P-ADOT, which can be considered the prototype of selective MT_2 antagonists. In contrast, a 3D-QSAR model built for non-selective melatonin receptor ligands[16] had revealed the presence of a favourite steric region near the 2-position of MLT, in the same plane of the indole, which can be occupied, for example, by the non-selective ligands 2-phenyl-MLT and **5j**. Therefore, the selectivity observed for **5e** and **11** could be due to the presence, in the MT_2 binding site, of an additional steric tolerance in a region different from the lipophilic pocket pointing towards the position 2 of the indole nucleus. The fact that the mt_1 receptor lacks this additional pocket could explain the affinity drop for the phenylalkyl groups on this subtype. The different receptor conformation that could be induced by substituent accommodation into the MT_2 binding site could be seen as a possible explanation for the loss of intrinsic activity on this receptor subtype.

Conclusions

The influence of substitutions at the C-2 indole position of indole melatonergic ligands on binding at both h-mt_1 and h-MT_2 receptors has been examined through QSAR studies (PLS and MRA methods). Substitution with electron-withdrawing substituents having an optimal lipophilicity (π value around 1), such as I, Br, COOMe, CF_3, resulted in a general increase in binding affinity. Compounds with hydrophilic substituents ($CONH_2$, $NHCONH_2$, CH_2OH) had lower affinity both for mt_1 and MT_2 receptors. In general, 2-substitution (**5a–d**, **5f–h**, **5j–k**) had a minimal effect on mt_1/MT_2 subtype selectivity. An interesting contrast between the effects of the C-2 substitution on subtype selectivity is found for 2-substitution with phenethyl, resulting in the compound (**5e**) with the highest MT_2/mt_1 selectivity ratio (ca. 50) among all of the ligands tested in this study; the introduction of a C-2 phenethyl group also causes a substantial decrease in intrinsic activity for the h-MT_2 receptor. These results suggest a different shape for the two binding pockets; the occupancy of the MT_2 putative cavity by an appropriately sized group could induce a different MT_2 receptor conformation responsible for the loss of intrinsic activity observed for **5e**.

Experimental

General

2-[^{125}I]Iodomelatonin (specific activity = 2000 Ci mmol^{-1}) and [^{35}S]-GTPγS (specific activity = 1070 mmol^{-1}) were purchased from Amersham (Bucks, UK). 2-Iodomelatonin was obtained from RBI (Natick, MA, USA). 2-Bromomelatonin,[19] 2-phenylmelatonin,[20] and the melatonergic derivatives **5a**,[26] **5i–k**[26] were synthesized as described elsewhere. Melting points were determined on a Büchi SMP-510 capillary melting point apparatus and are uncorrected. ^{1}H NMR spectra were recorded on a Bruker AC 200 spectrometer; chemical shifts (δ scale) are reported in parts per million (ppm) relative to the central peak of the solvent. Coupling constants (*J* values) are given in hertz (Hz). EI–MS spectra (70 eV) were taken on a Fisons Trio 1000. Only molecular ions (M^+) and base peaks are given. Infrared spectra were obtained on a Bruker FT-48 spectrometer; absorbances are reported in ν (cm^{-1}). Elemental analyses for C, H and N were performed on a Carlo Erba analyzer, and were within $\pm$0.4% of theoretical values.

6-Methoxy-2-methylthio-1*H*-indole. SO_2Cl_2 (0.8 mL, 10 mmol) was added to a cooled (−25 °C) solution of dimethyl disulphide (1.0 mL, 11 mmol) in CH_2Cl_2 (25 mL); the cooling was removed and the mixture was stirred and let warm to room temperature. 2.6 mL of this solution were added to a stirred solution of 6-methoxyindole[32] (0.294 g, 2 mmol) in CH_2Cl_2 (100 mL), and the mixture was stirred at room temperature for 5 min. The reaction mixture was washed with a 2 N Na_2CO_3 solution and, after drying over Na_2SO_4, the solvent was removed. The crude residue was filtered on silica gel (cyclohexane/EtOAC, 8:2) to give 0.29 g of a mixture of four products (starting material, two isomers of the thiomethyl derivative and a dithiomethyl derivative) detected by GC–MS (EI). This mixture was added to polyphosphoric acid (PPA) (20 g), preheated to 100 °C under mechanical stirring and a nitrogen atmosphere, and the mixture was stirred at 100 °C for 1 h. After cooling, water was added, the mixture was left under stirring for 30 min, and then extracted three times with ethyl acetate. After drying over Na_2SO_4 the solvent was

removed to give the crude 2-methylthio-6-methoxyindole that was purified by column flash chromatography (silica gel; cyclohexane–ethyl acetate, 8:2 as eluent) followed by crystallization from dichloromethane-cyclohexane (0.08 g, 21%). Mp 57 °C; ^{1}H NMR ($CDCl_3$): δ 2.47 (s, 3H), 3.85 (s, 3H), 6.55 (d, 1H, J = 1.4 Hz), 6.80 (m, 2H), 7.43 (d, 1H, J = 8.3 Hz), 8.03 (br s, 1H); EIMS m/z 193 (M^+), 178 (100); IR (cm^{-1}, nujol): 3395, 1621.

2-Methanesulfonyl-6-methoxy-1*H*-indole (2c). A solution of magnesium monoperoxyphtalate hexahydrate (MMPP 80%) (0.492 g, 0.99 mmol) and of benzyltriethylammonium chloride (0.015 g, 0.1 equiv) in water (5 mL) was added to a 0 °C cooled solution of 2-methylthio-6-methoxyindole (0.128 g, 0.66 mmol) in dichloromethane (10 mL). After stirring for 5 min, the layers were separated and the aqueous layer was extracted with dichloromethane. The combined organic layers were washed with a saturated $NaHCO_3$ solution and then with water. The organic phase was dried (Na_2SO_4), filtered, concentrated in vacuo and purified by flash chromatography (silica gel; cyclohexane/ethyl acetate, 8:2) followed by crystallization from ethyl acetate/cyclohexane, to yield 0.12 g (79%) of the desired product **2c**. Mp 137–138 °C; ^{1}H NMR ($CDCl_3$): δ 3.20 (s, 3H), 3.67 (s, 3H), 6.89 (m, 2H), 7.15 (d, 1H, J = 1.5 Hz), 7.58 (d, 1H, J = 9.4 Hz), 8.98 (br s, 1H); EIMS m/z 225 (M^+, 100); IR (cm^{-1}, nujol): 3296, 1621.

General procedure for the synthesis of (1*H*-indol-1-yl) acetonitrile derivatives (3a–d). A solution of the appropriate indole **2a**–**d** (10 mmol) in dry DMF (10 mL) was added dropwise to a stirred ice-cooled suspension of sodium hydride (0.42 g of an 80% dispersion in mineral oil, 14 mmol) in dry DMF (30 mL) under a N_2 atmosphere. After the addition, the mixture was stirred at 0 °C for 30 min, then chloroacetonitrile (1.06 g, 14 mmol) was added dropwise and the resulting mixture was stirred at room temperature for 16 h, then poured into ice-water (250 g) and extracted with ethyl acetate. The organic phase was washed with brine, dried over sodium sulphate and concentrated under reduced pressure to give a residue which was purified by flash column chromatography (silica gel; cyclohexane/ethyl acetate, 7:3 as eluent for **3a**–**b** and dichloromethane/ethyl acetate, 98:2 for **3c**–**d**) and crystallization.

1-Cyanomethyl-1*H*-indole-2-carboxylic acid methyl ester (3a). This was prepared as described in the literature.[26]

(6-Methoxy-2-trifluoromethyl-1*H*-indol-1-yl)acetonitrile (3b). White crystalline solid (3.92 g, 86%); mp 68–69 °C (Et_2O/hexane); ^{1}H NMR ($CDCl_3$): δ 3.93 (s, 3H), 5.06 (s, 2H), 6.83 (d, 1H, J = 2.0 Hz), 6.94 (dd, 1H, J = 2.0, 8.9 Hz), 6.99 (m, 1H), 7.58 (d, 1H, J = 8.9 Hz); EIMS m/z 254 (M^+), 214 (100); IR (cm^{-1}, nujol): 1627.

(2-Methanesulfonyl-6-methoxy-1*H*-indol-1-yl)acetonitrile (3c). White crystalline solid (1.82 g, 69%); mp 164 °C (EtOAc/cyclohexane); ^{1}H NMR ($CDCl_3$): δ 3.29 (s, 3H), 3.95 (s, 3H), 5.48 (s, 2H), 6.80 (d, 1H, J = 2.1 Hz), 6.97 (dd, 1H, J = 2.1, 8.9 Hz), 7.35 (s, 1H), 7.63 (d, 1H, J = 8.9 Hz), 9.76 (s, 1H); EIMS m/z 264 (M^+, 100); IR (cm^{-1}, nujol): 2259, 1621.

(2-Formyl-6-methoxy-1*H*-indol-1-yl)acetonitrile (3d). White crystalline solid (0.38 g, 18%); mp 152 °C (EtOAc/hexane); ^{1}H NMR ($CDCl_3$): δ 3.94 (s, 3H), 5.64 (s, 2H), 6.80 (d, 1H, J = 1.9 Hz), 6.93 (dd, 1H, J = 1.9, 8.8 Hz), 7.29 (s, 1H), 7.65 (d, 1H, J = 8.8 Hz), 9.76 (s, 1H); EIMS m/z 214 (M^+, 100); IR (cm^{-1}, nujol): 1658.

(6-Methoxy-2-styryl-1*H*-indol-1-yl)acetonitrile (4). Benzyltriphenylphosphonium chloride (0.23 g, 0.59 mmol) was added to a stirred solution of **3d** (0.09 g, 0.42 mmol) and DBU (0.12 mL) in toluene (9 mL) and the mixture was refluxed for 4 h. The mixture was cooled to room temperature, dichloromethane was added, and the organic phase was washed with water, dried (Na_2SO_4), and concentrated under reduced pressure to give the crude olefin **4** as a mixture of *E* and *Z* isomers. Purification by flash chromatography (silica gel; dichloromethane as eluent) gave 0.072 g (59.5% yield) of the stereoisomeric olefins which was used in the next step without further purification. EIMS m/z 288 (M^+, 100).

General procedure for the synthesis of 2-substituted-*N*-[2-(6-methoxy-1*H*-indol-1-yl)ethyl]propionamido derivatives (5a–c, e). A solution of the suitable indol-1-yl-acetonitrile **3a–c, 4** (1 mmol) in THF (5 mL) and propionic anhydride (2 mL) was hydrogenated for 6 h at 50 °C under pressure (4 atm) using Raney nickel as catalyst. Following catalyst removal (by filtration on Celite®), the evaporation of the solvent gave a residue which was partitioned between ethyl acetate and 2 N NaOH. The organic layer was washed with brine, dried (Na_2SO_4) and evaporated under reduced pressure to give crude title compounds (**5a**–**c**, **e**) which were purified by flash-chromatography (silica gel; cyclohexane/ethyl acetate, 3:7) and crystallization.

1-(2-Propionylamino-ethyl)-6-methoxy-1*H*-indol-1-yl-2-carboxylic acid methyl ester (5a). This was prepared as described in literature.[26]

***N*-[2-(6-Methoxy-2-trifluoromethyl-1*H*-indol-1-yl)ethyl]-propionamide (5b).** White crystalline solid (0.23 g, 73%); mp 100–101 °C (dichloromethane/hexane); ^{1}H NMR ($CDCl_3$): δ 1.12 (t, 3H), 2.16 (q, 2H), 3.64 (q, 2H), 3.91 (s, 3H), 4.36 (t, 2H), 5.57 (br t, 1H), 6.85 (dd, 1H, J = 2.0, 8.7 Hz), 6.90 (s, 1H), 7.03 (d, 1H, J = 2.0 Hz), 7.52 (d, 1H, J = 8.7 Hz); EIMS m/z 314 (M^+), 241 (100); IR (cm^{-1}, nujol): 3323, 1647. Anal. calcd for $C_{15}H_{17}F_3N_2O_2$ (314.31): C, 57.32; H, 5.45; N, 8.91. Found: C, 57.70; H, 5.48; N, 8.94.

***N*-[2-(2-Methanesulfonyl-6-methoxy-1*H*-indol-1-yl)ethyl] propionamide (5c).** White crystalline solid (0.22 g, 68%); mp 135 °C (ethyl acetate/cyclohexane); ^{1}H NMR ($CDCl_3$): δ 1.07 (t, 3H), 2.12 (q, 2H), 3.19 (s, 3H), 3.68 (m, 2H), 3.91 (s, 3H), 4.54 (t, 2H), 6.08 (br t, 1H), 6.87 (dd, 1H, J = 2.1, 8.8 Hz), 6.99 (d, 1H, J = 2.1 Hz), 7.21 (s, 1H), 7.55 (d, 1H, J = 8.8 Hz); EIMS m/z 324 (M^+), 251 (100); IR (cm^{-1}, nujol): 3367, 1639. Anal. calcd for $C_{15}H_{20}N_2SO_4$ (324.39): C, 55.54; H, 6.21; N, 8.64. Found: C, 55.94; H, 6.29; N, 8.62.

***N*-[2-(6-Methoxy-2-phenethyl-1*H*-indol-1-yl)ethyl]propionamide (5e).** Beige crystalline solid (0.29 g, 82%); mp 125 °C (EtOAc/cyclohexane); ^{1}H NMR ($CDCl_3$): δ 1.06 (t, 3H), 2.09 (q, 2H), 3.02 (m, 4H), 3.51 (m, 2H), 3.86 (s, 3H), 4.16 (t, 2H), 5.45 (br t, 1H), 6.28 (s, 1H), 6.75 (dd, 1H, J = 2.2, 8.4 Hz), 6.83 (d, 1H, J = 2.2 Hz), 7.22–7.32 (m, 5H), 7.42 (d, 1H, J = 8.4 Hz); EIMS m/z 350 (M^+), 259 (100); IR (cm^{-1}, nujol): 3309, 1642. Anal. calcd for $C_{22}H_{26}N_2O_2$ (350.46): C, 75.40; H, 7.48; N, 7.99. Found: C, 75.15; H, 7.56; N, 8.04.

1-(2-Propionylamino-ethyl)-6-methoxy-1*H*-indol-1-yl-2-carboxylic acid (6). A solution of **5a**[26] (3.04 g, 10 mmol) in THF (20 mL), MeOH (24 mL) and 3 N KOH (10 mL) was stirred at room temperature for 16 h. After cooling to 0 °C, the solution was acidified with 6 N HCl and the white solid that precipitated was collected, washed with water, and dried at 50 °C under vacuum to give 2.64 g (91%) of the acid **6** which was directly used without further purification. Mp 204 °C; ^{1}H NMR (DMSO-d_6): δ 0.87 (t, 3H), 1.92 (q, 2H), 3.36 (q, 2H), 3.81 (s, 3H), 4.54 (t, 2H), 6.75 (dd, 1H, J = 2.1, 8.8 Hz), 7.07 (d, 1H, J = 2.1 Hz), 7.15 (s, 1H), 7.51 (d, 1H, J = 8.8 Hz), 7.90 (br t, 1H), 12.70 (br s, 1H); EIMS m/z 290 (M^+), 217 (100); IR (cm^{-1}, nujol): 3260, 1664.

1-(2-Propionylamino-ethyl)-6-methoxy-1*H*-indol-1-yl-2-carboxylic acid amide (5f). Thionyl chloride (0.08 mL) was added to a solution of the acid **6** (0.18 g, 0.62 mmol) in dry THF (10 mL) and the mixture was stirred at room temperature for 15 min under nitrogen, then heated at 50 °C for 4 h, and finally allowed to stand at room temperature for 2 h. The solvent and excess thionyl chloride were removed under reduced pressure and the residue was dissolved in dry THF (40 mL). A saturated solution of ammonia in dichloromethane was poured into the ice-cooled solution of the acid chloride and the mixture was stirred at room temperature for 2 h. Petroleum ether was added to the reaction mixture and the yellow solid that precipitated upon cooling to 0 ° C was collected, washed with water, and dried (0.15 g; yield 85%). An analytical sample of **5f** was prepared by recrystallization from methanol. Mp 206–207 °C; ^{1}H NMR (DMSO-d_6): δ 0.83 (t, 3H), 1.96 (q, 2H), 3.69 (q, 2H), 3.78 (s, 3H), 4.50 (t, 2H), 6.71 (dd, 1H, J = 2.0, 8.7 Hz), 6.99 (s, 1H), 7.07 (s, 1H), 7.25, 7.87 (2 br s, 2H exchangeable), 7.46 (d, 1H, J = 8.7 Hz), 7.99 (br t, 1H); EIMS m/z 289 (M^+), 174 (100); IR (cm^{-1}, nujol): 3290, 3149, 1679. Anal. calcd for $C_{15}H_{19}N_3O_3$ (289.33): C, 62.27; H, 6.62; N, 14.52. Found: C, 62.02; H, 6.60; N, 14.35.

1-(2-Propionylamino-ethyl)-6-methoxy-1*H*-indol-1-yl-2-carbonyl azide (7). Diphenyl phosphorazidate (0.18 mL, 0.83 mmol) was added to a solution of **6** (0.2 g, 0.69 mmol) in benzene (5 mL) and Et_3N (0.14 mL) and the reaction mixture was stirred for 24 h at room temperature under nitrogen. The resulting suspension was dissolved in ethyl acetate, washed sequentially with water and a saturated $NaHCO_3$ aqueous solution, and dried (Na_2SO_4). The solvent was removed under reduced pressure to give the crude product **7** (0.21 g, 97%) that was used in the next step without further purification.

^{1}H NMR ($CDCl_3$): δ 1.07 (t, 3H), 2.12 (q, 2H), 3.67 (m, 2H), 3.91 (s, 3H), 4.66 (t, 2H), 5.84 (br t, 1H), 6.83 (dd, 1H, J = 2.4, 8.8 Hz), 6.85 (d, 1H, J = 2.4 Hz), 7.35 (s, 1H), 7.53 (d, 1H, J = 8.8 Hz); EIMS m/z 315 (M^+), 32 (100); IR (cm^{-1}, nujol): 3311, 2151, 1663.

***N*-[2-(6-Methoxy-2-ureido-1*H*-indol-1-yl)ethyl]propionamide (5g).** Ammonium acetate (0.15 g, 1.9 mmol) was added to a solution of **7** (0.21 g, 0.66 mmol) in toluene (15 mL) and the mixture was heated at reflux for 5 min under nitrogen. The mixture was cooled to room temperature, the solid filtered, washed sequentially with toluene, water and diethyl ether, and dried in vacuo to give 0.11 g (54%) of the ureido product **5g** as a white solid. An analytical sample was obtained by crystallization from ethyl acetate/methanol. Mp 191 °C; ^{1}H NMR (DMSO-d_6): δ 0.90 (t, 3H), 1.98 (q, 2H), 3.30 (m, 2H), 3.72 (s, 3H), 4.03 (t, 2H), 6.03 (br s, 2H, exchangeable with D_2O), 6.14 (s, 1H), 6.62 (dd, 1H, J = 2.2, 8.4 Hz), 6.97 (d, 1H, J = 2.2 Hz), 7.27 (d, 1H, J = 8.4 Hz), 7.93 (br t, 1H, exchangeable with D_2O), 8.17 (br s, 1H, exchangeable with D_2O); EIMS m/z 304 (M^+), 188 (100); IR (cm^{-1}, nujol): 3453, 3288, 1668, 1636. Anal. calcd for $C_{15}H_{20}N_4O_3 \cdot 0.6H_2O$ (315.16): C, 57.17; H, 6.78; N, 17.78. Found: C, 56.94; H, 6.39; N, 17.46.

***N*-[2-(2-Hydroxymethyl-6-methoxy-1*H*-indol-1-yl) ethyl]-propionamide (5h).** A solution **5a**[26] (0.73 g, 2.4 mmol) in dry THF (8 mL) was added dropwise to a stirred suspension of $LiAlH_4$ (0.11 g) in dry THF (5 mL) at 0 °C under nitrogen. The mixture was stirred for additional 1 h at 10 °C, and the unreacted $LiAlH_4$ was destroyed by careful addition of water. The resulting mixture was filtered through a Celite® pad and the filtrate was dried over Na_2SO_4. The dried solution was concentrated under reduced pressure to give a crude oil. Purification of the oil by filtration on silica gel (ethyl acetate as eluent) gave 0.60 g (91% yield) of **5h** as orange viscous oil. ^{1}H NMR ($CDCl_3$): δ 1.05 (t, 3H), 2.12 (q, 2H), 3.68 (q, 2H), 3.88 (s, 3H), 4.31 (t, 2H), 4.79 (s, 2H), 6.15 (br t, 1H), 6.42 (d, 1H, J = 0.6 Hz), 6.78 (dd, 1H, J = 2.2, 8.6 Hz), 6.84 (d, 1H, J = 2.2 Hz), 7.46 (dd, 1H, J = 8.6, 0.6 Hz); EIMS m/z 276 (M^+), 160 (100); IR (cm^{-1}, nujol): 3327, 2925, 1647. Anal. calcd for $C_{15}H_{20}N_2O_3$: (276.34) C, 65.20; H, 7.30; N, 10.14. Found: C, 65.34; H, 6.93; N, 9.78.

***N*-[2-(2-Formyl-6-methoxy-1*H*-indol-1-yl)ethyl]propionamide (5d).** Activated manganese dioxide (0.6 g) was added to a solution of **5h** (0.414 g, 1.5 mmol) in dry dichloromethane (15 mL). The mixture was stirred for 10 h at room temperature and then filtered. The filter cake was washed with hot acetone (4×8 mL), and the combined filtrates were concentrated under reduced pressure to yield 0.42 g of a crude orange oil. Purification of the crude product by flash column chromatography (silica gel; cyclohexane/ethyl acetate, 3:7) afforded 0.1 g (24%) of **5d** as white solid, and 0.29 g (70%) of the unreacted starting material **5h**. Mp 120–121 °C (dichloromethane/hexane); ^{1}H NMR ($CDCl_3$): δ 1.07 (t, 3H), 2.11 (q, 2H), 3.67 (q, 2H), 3.91 (s, 3H), 4.66 (t, 2H), 5.98 (br t, 1H), 6.82–7.61 (m, 4H), 9.72 (s, 1H);

EIMS m/z 274 (M^+), 201 (100); IR (cm^{-1}, nujol): 1659. Anal. calcd for $C_{15}H_{18}N_2O_3$: (274.32) C, 65.68; H, 6.61; N, 10.21. Found: C, 65.34; H, 6.23; N, 10.10.

Pharmacological evaluation

Membrane preparation. The preparation of membranes was described elsewhere.[28,37] In short, NIH3T3 cells stably expressing the cloned human mt_1 or MT_2 receptor subtypes were grown to confluence. On the day of assay the cells were detached from the flasks with ethylenediaminetetracetic acid (EDTA) (4 mM)/Tris–HCl (50 mM), pH 7.4, room temperature, and collected by centrifugation at $1000\times g$ for 10 min at 4 °C. The cells were suspended in EDTA (2 mM)/Tris–HCl (50 mM), homogenized in 10–15 volumes of ice-cold EDTA (2 mM)/Tris–HCl (50 mM) with an ultra-Turrax apparatus and centrifuged at $50{,}000\times g$ at 4 °C for 25 min. The final pellet was then resuspended in ice-cold Tris–HCl (50 mM) assay buffer.

Membrane protein level was determined according to a previously reported method.[38]

2-[^{125}I]Iodomelatonin binding assays. Affinities of compounds were determined in competition binding assays, by the displacement of 2-[^{125}I]iodomelatonin from mt_1 and MT_2 receptors expressed in NIH3T3 cells.

2-[^{125}I]Iodomelatonin (100 pM) and a range of concentrations of test compound were incubated with the receptor preparation for 90 min at 37 °C. The final membrane concentration was 5–10 μg protein per tube. The binding conditions were described in detail elsewhere.[39] IC_{50} values were determined by non linear fitting strategies and pK_i values were calculated from the IC_{50} values using the Cheng–Prusoff equation.[40] In saturation studies 2-[^{125}I]iodomelatonin was added at concentrations ranging from 10 to 1000 pM.

Determination of the intrinsic activity: [^{35}S]GTPγS binding assays. [^{35}S]GTPγS Binding studies in NIH3T3 cells expressing human cloned mt_1 or MT_2 receptors were performed as previously described.[25,28,37] The final pellet, obtained as described above (membrane preparation), was resuspended in ice-cold Tris–HCl assay buffer (50 mM) to give a final membrane concentration of 20–30 mg/mL. The membranes (15–25 μg of protein) were then incubated at 30 °C for 30 min in the presence and in the absence of melatonin analogues, in an assay buffer consisting of [^{35}S]GTPγS (0.3–0.5 nM), GDP (50 μM), NaCl (100 mM) and $MgCl_2$ (3 mM). The final incubation volume was 100 μL. The incubation was terminated by the addition of ice-cold Tris–HCl buffer, pH 7.4 (1 mL), rapid vacuum filtration through Whatman GF/B glass-fiber filters followed by three (3 mL) washes with ice-cold Tris–HCl buffer, pH 7.4. Bound radioactivity was determined by liquid scintillation spectrophotometry after overnight extraction in 4 mL Filter-Count scintillation fluid. Basal binding was assessed in the absence of ligands, and non-specific binding was defined using GTPγS (10 μM). Basal stimulation is the amount of [^{35}S]GTPγS specifically bound in the absence of compounds and was taken as 100%. The maximal G-protein activation was measured in each experiment by using MLT (100 nM). Compounds were added to a concentration equivalent to 100 nM of MLT, and the percent stimulation above basal was determined. The equivalent concentration was estimated on the basis of the ratio of the affinity of the test compound over that of MLT. It was assumed that at the equivalent concentration the test compound occupies the same number of receptors as MLT 100 nM. All measurements were performed in triplicate. The SEM values were below 15% of the mean.

Melatonin caused a 370% increase over basal (100%) [^{35}S]GTPγS binding in NIH3T3 expressing the mt_1 receptor and 250% increase in NIH3T3 expressing the MT_2 receptor. The relative intrinsic activity values were obtained by dividing the maximal G-protein activation of a test compound by that of MLT. Thus the relative intrinsic activity of MLT is always 1, for partial agonists between 0 and 1 and for antagonists 0.

Experimental design for substituent selection

For a set of 59 substituents, a large number of structural descriptors has been reported,[41] and a smaller set of principal properties, named disjoint principal properties (DPP), has been derived from separate groups of descriptors.[29] These DPPs are classified into three groups, containing information on the steric (s), electronic (e), lipophilic (l) and hydrogen-bonding properties of the substituents; due to the method of calculation, they are not mutually orthogonal, but their chemical meaning is clear, and their ability to condense information from several descriptors makes them useful for compound selection in experimental design.

The substituents to be introduced in position 2 of the indole ring were selected on the basis of the first steric (S_1), electronic (E_1) and lipophilic (L_1) DPPs, through an iterative procedure employing the program DESDOP.[42] This program calculates an index, called D-efficiency, based on the determinant of the X′X matrix, and related to both the volume occupied by the substituents in the property space, and to inter-property correlation.[43] During the selection procedure, some reaction-based and knowledge-based constraints were taken in account. Some substituents which could present synthetic difficulty were in fact excluded from the experimental domain, while some others, known to grant good affinity when introduced on the MLT structure (i.e., Ph, Br, COOMe),[16] were forced into the selection. As the effect of 2-alkyl substituents on MLT binding affinity had been previously investigated,[20] and it was found to be detrimental for receptor affinity, the presence of alkyl groups was limited to the phenethyl one. This group also represented the upper limit of lipophilicity and steric hindrance for the present study.

The correlation matrix for compounds **5a**–**k**, reported in Table 2, shows low correlation between couples of the first three DPP.

QSAR

QSARs were analyzed expressing the affinity for each receptor subtype as a contribution of the substituent, relative to that of the unsubstituted compound $\left(K_i^X/K_i^H\right)$. The −log of relative affinity was indicated as pRA. Therefore, $pRA(R_1=X)=pK_i(R_1=X)-pK_i(R_1=H)$ both for compounds **5a**–**k** and for MLT derivatives **8**–**11**. Relative affinities for the mt_1 and MT_2 receptors are indicated as pRA1 and pRA2, respectively. pRA values for compounds **5a**–**k**, and for MLT derivatives **8**–**11**, are reported in Table 3.

Structural descriptors used for regression analyses were selected from the databank compiled by van de Waterbeemd et al., which can be downloaded from the web site of the QSAR and Modeling Society (www.pharma.ethz.ch/qsar/). Detailed description of the variables can be found in the original paper.[29] A limited set of substituent constants, reported in Table 4, was employed, to avoid an excessive risk of chance correlation.

Multiple regression analysis (MRA) was performed by Excel,[44] using an in-house macro routine to provide all the possible combinations of a certain number of variables. Partial least squares (PLS) models were calculated, after scaling of the variables to unit variance, with the program Simca 6.0.[45] The lipophilicity variable (π) was squared, in order to include parabolic effects. The descriptive power of the models are estimated by R^2Y, expressing the fraction of the variance of the Y matrix explained by the latent variables, and by R^2X, expressing the same for the X matrix. Cross validation excluding one compound at a time (leave-one-out method) was employed to calculate Q^2 values ($Q^2=1-PRESS/SSy$, where PRESS is the sum of squares of the residuals in prediction, i.e., for the compounds excluded from the training set, and SSy is the sum of squares of the deviations from the mean value of y), as an estimate of the predictive power of the models. The standard deviation of the errors in prediction (SDEP) was calculated as (PRESS/N)_, where N is the total number of compounds.

Conformational analysis and conformer superposition

Molecular modeling studies were performed with the Sybyl 6.6 software[46] running on a Silicon Graphics O2 workstation. Three-dimensional models of the molecules were energy-minimized using the standard Tripos force field,[47] ignoring the electrostatic contribution, to an energy gradient of 0.01 Kcal/mol·Å, with the Powell method.

Compounds **11** and **5e** were submitted to a systematic conformational search (Systematic Search routine of Sybyl) to generate the conformations having different orientations of the side chains in position 2. The methoxy group and the acylaminoethyl side chain were kept in a conformation corresponding to the pharmacophore model previously described (model B in ref 23), while the two single bonds in the benzyl group of **11** and the three single bonds in the phenethyl group of **5e** were rotated by steps of 30°. An energy filter of 100 Kcal/mol was applied, in order to reduce the number of conformations, and each of the conformers thus obtained was energy-minimized. The six conformers obtained for **11**, and the 16 for **5e**, were submitted to the following analysis.

For each conformer the distances between the centroid of the phenyl ring in position 2 and three key features of the molecule were measured, that is (1) the carbonyl oxygen of the amide group; (2) the hydrogen atom of the amide group; (3) the centroid of the benzene fragment of the indole ring. The three distances found for each conformer of **11** were compared to those measured for the conformers of **5e**. The couples of conformers having differences, in all the distances, lower than 1 Å were mutually superposed fitting the putative pharmacophore elements, that is the methoxy oxygen, the benzene fragment of the indole nucleus, the four atoms of the amide group and the centroid of the phenyl ring of the 2-substituent.

Acknowledgements

This work was supported by grants from Ministero dell'Università e della Ricerca Scientifica e Tecnologica (MURST) and University of Urbino. We thank Mr. Francesco Palazzi for technical assistance.

References

1. Reiter, R. J. *Endocr. Rev.* **1991**, *12*, 151.
2. Bubenik, G. A.; Blask, D. E.; Brown, G. M.; Maestroni, G. J.; Pang, S. F.; Reiter, R. J.; Viswanathan, M.; Zisapel, N. *Biol. Signals Recept.* **1998**, *7*, 195.
3. Zhdanova, I. V.; Wurtman, R. J.; Lynch, H. J.; Ives, J. R.; Dollins, A. B.; Morabito, C.; Matheson, J. K.; Schomer, D. L. *Clin. Pharmacol. Ther.* **1995**, *57*, 552.
4. Arendt, J.; Deacon, S. *Chronobiol. Int.* **1997**, *14*, 185.
5. Arendt, J.; Skene, D. J.; Middleton, B.; Lockley, S. W.; Deacon, S. *J. Biol. Rhythms* **1997**, *12*, 604.
6. Van Reeth, O. *Horm. Res.* **1998**, *49*, 158.
7. Oldani, A.; Ferini-Strambi, L.; Zucconi, M.; Stankov, B.; Fraschini, F.; Smirne, S. *NeuroReport* **1994**, *6*, 132.
8. Arangino, S.; Cagnacci, A.; Angiolucci, M.; Vacca, A. M.; Longu, G.; Volpe, A.; Melis, G. B. *Am. J. Cardiol.* **1999**, *83*, 1417.
9. Ebisawa, T.; Karne, S.; Lerner, M. R.; Reppert, S. M. *Proc. Natl. Acad. Sci. U.S.A.* **1994**, *91*, 6133.
10. Reppert, S. M.; Weaver, D. R.; Ebisawa, T. *Neuron* **1994**, *13*, 1177.
11. Reppert, S. M.; Godson, C.; Mahle, C. D.; Weaver, D. R.; Slaugenhaupt, S. A.; Gusella, J. F. *Proc. Natl. Acad. Sci. U.S.A.* **1995**, *92*, 8734.
12. Mazzucchelli, C.; Pannacci, M.; Nonno, R.; Lucini, V.; Fraschini, F.; Stankov, B. M. *Mol. Brain Res.* **1996**, *39*, 117.
13. Dubocovich, M. L.; Cardinali, D. P.; Hagan, R. M.; Krause, D. N.; Sudgen, D.; Vanhoutte, P. M.; Yocca, F. D. In *The IUPHAR Compendium of Receptor Characterization and Classification*; Girdlestone D., Ed.; IUPHAR Media: London, 1998, pp 187–193.
14. Mathé-Allainmat, M.; Andriex, J.; Langlois, M. *Exp. Opin. Ther. Patents* **1997**, *7*, 1447.
15. Mor, M.; Plazzi, P. V.; Spadoni, G.; Tarzia, G. *Curr. Med. Chem.* **1999**, *6*, 501.

16. Mor, M.; Rivara, S.; Silva, C.; Bordi, F.; Plazzi, P. V.; Spadoni, G.; Diamantini, G.; Balsamini, C.; Tarzia, G.; Fraschini, F.; Lucini, V.; Nonno, R.; Stankov, B. M. *J. Med. Chem.* **1998**, *41*, 3831.
17. Spadoni, G.; Balsamini, C.; Bedini, A.; Carey, A.; Diamantini, G.; Di Giacomo, B.; Tontini, A.; Tarzia, G.; Nonno, R.; Lucini, V.; Pannacci, M.; Stankov, B. M.; Fraschini, F. *Med. Chem. Res.* **1998**, *8*, 487.
18. Takaki, K. S.; Mahle, C. D.; Watson, A. J. *Curr. Pharm. Des.* **1997**, *3*, 429.
19. Duranti, E.; Stankov, B.; Spadoni, G.; Duranti, A.; Lucini, V.; Capsoni, S.; Biella, G.; Fraschini, F. *Life Sci.* **1992**, *51*, 479.
20. Spadoni, G.; Stankov, B.; Duranti, A.; Biella, G.; Lucini, V.; Salvatori, A.; Fraschini, F. *J. Med. Chem.* **1993**, *36*, 4069.
21. Garratt, P. J.; Jones, R.; Rowe, S. J.; Sugden, D. *Bioorg. Med. Chem. Lett.* **1994**, *4*, 1555.
22. Garratt, P. J.; Vonhoff, S.; Rowe, S. J.; Sugden, D. *Bioorg. Med. Chem. Lett.* **1994**, *4*, 1559.
23. Spadoni, G.; Balsamini, C.; Diamantini, G.; Di Giacomo, B.; Tarzia, G.; Mor, M.; Plazzi, P. V.; Rivara, S.; Lucini, V.; Nonno, R.; Pannacci, M.; Fraschini, F.; Stankov, B. M. *J. Med. Chem.* **1997**, *40*, 1990.
24. Dubocovich, M. L.; Masana, M. I.; Iacob, S.; Sauri, D. M. *Naunyn-Schmiedeberg's Arch. Pharmacol.* **1997**, *355*, 365.
25. Spadoni, G.; Balsamini, C.; Bedini, A.; Diamantini, G.; Di Giacomo, B.; Tontini, A.; Tarzia, G.; Mor, M.; Plazzi, P. V.; Rivara, S.; Nonno, R.; Pannacci, M.; Lucini, V.; Fraschini, F.; Stankov, B. M. *J. Med. Chem.* **1998**, *41*, 3624.
26. Tarzia, G.; Diamantini, G.; Di Giacomo, B.; Spadoni, G.; Esposti, D.; Nonno, R.; Lucini, V.; Pannacci, M.; Fraschini, F.; Stankov, B. M. *J. Med. Chem.* **1997**, *40*, 2003.
27. Sugden, D.; Pickering, H.; Teh, M.-T.; Garrattt, P. J. *Biol. Cell* **1997**, *89*, 531.
28. Nonno, R.; Lucini, V.; Pannacci, M.; Mazzucchelli, C.; Angeloni, D.; Fraschini, F.; Stankov, B. M. *Br. J. Pharmacol.* **1998**, *124*, 485.
29. van de Waterbeemd, H.; Costantino, G.; Clementi, S.; Cruciani, G.; Valigi, R. Disjoint Principal Properties of Organic Substituents. In *Chemometric Methods in Molecular Design*; Mannhold, R., Krogsgaard-Larsen, P., Timmerman, H., Eds.; VCH: Weinheim/New York, 1995; pp 103–111.
30. Mager, P. P. *Med. Res. Rev.* **1997**, *17*, 453.
31. Box, G. E. P.; Hunter, W. G., Hunter, J. S. *Statistics for Experimenters*; Wiley: New York, 1978; pp 306–373.
32. Allen, M. S.; Hamaker, L. K.; La Loggia, A. J.; Cook, J. M. *Synth. Commun.* **1992**, *22*, 2077.
33. Miyashita, K.; Kondoh, K.; Tsuchiya, K.; Miyabe, H.; Imanishi, T. *J. Chem. Soc. Perkin Trans. 11* **1996**, 1261.
34. Dillard, R. D.; Bach, N. J.; Draheim, S. E.; Berry, D. R.; Carlson, D. G.; Chirgadze, N. Y.; Clawson, D. K.; Hartley, L. W.; Johnson, L. M.; Jones, N. D.; McKinney, E. R.; Mihelic, E. D.; Olkowski, J. L.; Schevitz, R. W.; Smith, A. C.; Snyder, D. W.; Sommers, C. D.; Wery, J.-P. *J. Med. Chem.* **1996**, *39*, 5119.
35. Wittig, G.; Schöllkopf, U. *Chem. Ber.* **1954**, *87*, 1318.
36. Noguchi, N.; Kuroda, T.; Hatanaka, M.; Ishimaru, T. *Bull. Chem. Soc. Jpn.* **1982**, *55*, 633.
37. Nonno, R.; Pannacci, M.; Lucini, V.; Angeloni, D.; Fraschini, F.; Stankov, B. M. *Br. J. Pharmacol.* **1999**, *127*, 1288.
38. Bradford, M. M. *Anal. Biochem.* **1976**, *72*, 248.
39. Stankov, B.; Cozzi, B.; Lucini, V.; Fumagalli, P.; Scaglione, F.; Fraschini, F. *Neuroendocrinology* **1991**, *53*, 214.
40. Cheng, Y.-C.; Prusoff, W. H. *Biochem. Pharmacol.* **1973**, *22*, 3099.
41. Van de Waterbeemd, H.; Testa, B. *Adv. Drug Res.* **1987**, *16*, 85.
42. *DESDOP*, v. 2.0; MIA srl: Perugia, Italy.
43. Baroni, M.; Clementi, S.; Cruciani, G.; Kettaneh-Wold, K.; Wold, S. D. *QSAR* **1993**, *12*, 225.
44. *Excel 97*; Microsoft Corp., 1997.
45. *Simca-S 6.01*; Umetri AB & Ericsson AB, 1997.
46. *Sybyl*, v. 6.6; Tripos Inc.: 1699 South Hanley Rd., St. Louis, MO 63144, USA, October 1999.
47. Clark, M.; Cramer, R. D., III; Van Opdenbosch, N. *J. Comp. Chem.* **1989**, *10*, 982.